archives
of thermodynamics
Vol. **37**(2016), No. 4, 137–159
DOI: 10.1515/aoter-2016-0032

Performance analyses of helical coil heat exchangers. The effect of external coil surface modification on heat exchanger effectiveness

RAFAŁ ANDRZEJCZYK
TOMASZ MUSZYŃSKI*

Gdańsk University of Technology, Narutowicza 11/12, 80-233 Gdańsk, Poland

Abstract The shell and coil heat exchangers are commonly used in heating, ventilation, nuclear industry, process plant, heat recovery and air conditioning systems. This type of recuperators benefits from simple construction, the low value of pressure drops and high heat transfer. In helical coil, centrifugal force is acting on the moving fluid due to the curvature of the tube results in the development. It has been long recognized that the heat transfer in the helical tube is much better than in the straight ones because of the occurrence of secondary flow in planes normal to the main flow inside the helical structure. Helical tubes show good performance in heat transfer enhancement, while the uniform curvature of spiral structure is inconvenient in pipe installation in heat exchangers. Authors have presented their own construction of shell and tube heat exchanger with intensified heat transfer. The purpose of this article is to assess the influence of the surface modification over the performance coefficient and effectiveness. The experiments have been performed for the steady-state heat transfer. Experimental data points were gathered for both laminar and turbulent flow, both for co current- and countercurrent flow arrangement. To find optimal heat transfer intensification on the shell-side authors applied the number of transfer units analysis.

Keywords: Effectiveness; Heat transfer intensification; Number of transfer unit; Helical coil

*Corresponding Author. E-mail: tommuszy@pg.gda.pl

Nomenclature

A	–	heat transfer surface area, m^2
B	–	outside diameter of inner cylinder, m
C	–	inner shell diameter, m
C_{co}	–	contraction coefficient
C_D	–	drag coefficient
c_p	–	specific heat, J/kgK
D	–	Dean number
D_e	–	shell side equivalent diameter, m
D_H	–	average diameter of helix, m
D_0	–	outside tube coil diameter, m
d_0	–	internal tube coil diameter, m
E	–	coefficient in Mishra and Gupta equation, m
g	–	gravitational acceleration, m/s^2
G	–	mass flow rate, kg/m^2s
HTC	–	heat transfer coefficient
HX	–	heat exchangers
f	–	friction factor
F	–	fluid correction factor
H	–	height of shell, m
L	–	length of coil, m
LMTD	–	logarithmic mean temperature difference
m	–	mass flow , kg/s
N	–	number of turns of helicail coil
NTU	–	number of transfer units
Nu	–	Nusselt number
p	–	distance between consecutive coil turns, m
Pr	–	Prandtl number
ΔP	–	pressure drop, Pa
$\dot{Q}$	–	heat flux, W
q_w	–	wall heat flux, W/m^2
Ra	–	Rayleigh number
R	–	fouling factor, m^2K/W
r	–	piper radius, m
Re	–	Reynolds number
T	–	temperature, K
U	–	overall heat transfer coefficient, W/m^2K
w	–	velocity, m/s
W	–	fluid heat capacity rate, W/K
$\dot{V}$	–	volumetric flow, m^3/s

Greek symbols

α	–	heat transfer coefficient, w/m^2K
δ	–	wall thickness, m
γ	–	area ratio
ρ	–	density, kg/m^3

ζ – friction factor for components
ε – heat exchanger effectiveness
ψ_s – separated flow multiplier
λ – thermal conductivity, W/mK
μ – dynamic viscosity, Pa s
ν – kinematic viscosity, m^2/s

Subscripts

av – average
c – cold
cor – corrected
$c-a$ – average at coil side
$c-s$ – coil side
con – contraction
CU – copper
exp – expansion
h – hot
$i0$ – internal
min – minimum
max – maximum
$s-a$ – average at shell side
s – surface
sh – shell side
t – tube
w – wall

1 Introduction

Striving to ensure high performance of the heat exchangers, HX, nowadays is a source of universal trend both to the miniaturization of these devices for both industrial and domestic applications, while maintaining the highest possible size to thermal energy ratio. As is well known, in the case of recuperators the heat transfer coefficient has a decisive influence on their efficiency [1]. Overall heat transfer coefficient, depends mainly on the lower value of heat transfer value (HTC) from working media [2]. It is, therefore, most significant to improve the heat transfer with special attention on the side of the medium with lower heat transfer coefficient [3].

Helical coils are widely used in applications such as heat recovery systems, chemical processing, food processing, nuclear reactors, and high-temperature gas cooling reactors. Helical coils have been widely studied both experimentally [4] and numerically [5].

Helical coils are characterized by their compactness and high heat transfer coefficient. When fluid flows through a helically coiled tube, the cur-

vature of the coil induces centrifugal force, causing the development of the secondary flow. This secondary flow enhances fluid mixing and thus heat transfer. Fluid flow in a helical tube is characterized by the Dean number. The Dean number, D, is a measure of the geometric average of inertial and centrifugal forces to the viscous force ratio, and thus is a measure of a magnitude of the secondary flow. For laminar flow and small pipe to coil radius aspect ratio r/R, frictional loss in a curved tube may be represented as a function of the Dean number. One of the most frequent uses of helically coiled tubes is in the shell and coiled tube heat exchangers.

The majority of the studies related to helically coiled tubes and heat exchangers have dealt with two major boundary conditions, i.e., constant heat flux and constant wall temperature [6,7]. However, these boundary conditions are not encountered in most single-phase heat exchangers.

Naphon [8] has investigated thermal performance of helical coils with and without fins. Two different coil diameters with 9.5 mm diameter copper tube having thirteen turns were used. Hot and cold water were used as working fluid in the range from 0.10 to 0.22 kg/s and from 0.02 to 0.12 kg/s, respectively. They have shown that with increasing hot water mass flow rate the friction factor decreased.

Various helical coils made from a 12.5 mm ID (inside diameter) tube with various coil diameters ranging from 92 to 1282 mm have been investigated by Srinivasan *et al.* [9] to determine friction factors. Four different coil pitches of 2.5, 3.3, 6.6, and 13.2 tube diameters were tested and graphs of friction factors with respect to the Dean number were produced. All the graphs showed breakpoints which were interpreted as the critical Reynolds number value so that equation was found to describe this critical value for different tube diameter to shell diameter ratio.

Kumar *et al.* [10] studied a tube-in-tube helically coiled heat exchanger for turbulent flow regime. Numerical investigations were done to understand forced laminar fluid flow in rectangular coiled pipes with circular cross-section by Conte and Peng [11]. Their focus was addressed on exploring the flow pattern and temperature distribution through the pipe.

Patankar *et al.* [12] discussed the effects of the Dean number on friction factor and heat transfer in the developing and fully developed regions of helically coiled pipes. Comparisons between the proposed model and the experiment showed good agreement. However, the effects of the torsion and the Prandtl number were not taken into account in the aforementioned model.

Jamshidi *et al.* [13] experimentally considered the effects of the geometric parameters to enhance the heat transfer rate in the shell and coiled-tube heat exchangers. The results indicated that the higher coil diameter, coil pitch, and mass flow rate in the shell and tube can enhance the heat transfer rate in these types of heat exchangers. Xin *et al.* [14] studied single-phase flow in a helical double tube heat exchanger in horizontal and vertical arrangements. In their paper, the influence of coil geometry, the flow rate of air and water on the pressure drop of single phase flow was surveyed.

Petrakis and Karahalios [15,16] obtained the numerical solution of incompressible viscous fluid flow equation for water flowing in a curved double tube with circular cross section. In this investigation, it was indicated that in small core radius, the change of Dean number has a considerable effect on fluid properties whereas it was not observed in the large radius.

Di Liberto and Ciofalo [17] studied the heat transfer of turbulent flow in curved tubes by numerical simulation. They also used this method to survey a fully developed turbulent flow in curved tubes. Results of this study indicated that in the curved tubes, the temperature fluctuations in outer regions are more pronounced than in other regions.

Moawed [18] reported an experimental investigation of steady-state natural convection heat transfer from uniformly heated helicoidal pipes oriented vertically and horizontally. His experimental investigation was conducted on four helicoidal pipes having different ratios of coil diameter to pipe diameter, pitch to pipe diameter and length to pipe diameter with the range of Rayleigh number $1.5 \times 10^3 < \mathrm{Ra} < 1.1 \times 10^5$. His results showed that the overall Nusselt number increases with the increase of coil to tube diameter ratio, dimensional pitch and length of coil to tube diameter for the vertical helicoidal pipes. For the horizontal helicoidal pipes, the overall Nusselt number increased with the increase of dimensional pitch and length of coil to tube diameter, but it decreased with the increase of coil to tube diameter ratio. He presented two different equations to correlate the Nusselt number for horizontal and vertical helicoidal pipes.

Literature review, reveals that there are a few investigations on the heat transfer coefficients of helical coil heat exchangers considering the geometrical effects and coil surface modifications. Also, this scarcity is more prominent for the shell-side heat transfer coefficients. Most of the researchers performed their work on the helically coiled heat exchanger with constant heat flux and constant wall temperature as major boundary conditions.

The paper presents labor that was carried out in several stages. The

first part of this paper presents the construction of the test facility and the design and construction of test exchangers. The second part presents experiments which were carried out on single-phase convection heat transfer with distilled water as a working medium.

2 Heat exchanger modeling

In order to conduct experimental research to verify the influence of the surface modification on the heat transfer coefficient of the coiled tube a reference heat exchanger model was proposed. Heat transfer coefficient outside the coil was calculated based on the works of methodology showed earlier in the literature [19,20]. Helically coiled tubes show some peculiar characteristics and phenomenological aspects of the thermohydraulics that are worthy of a brief description. First of all, coiled pipes are compact, can well accommodate the thermal expansions and have a high resistance to flow induced vibrations [21,22]. Furthermore, the fluid flowing in helical tubes develops secondary flows whose physical explanation is represented in Fig. 1. The curved shape of the inner tube of HX causes the fluid to experience a centrifugal force which depends on its local axial velocity of Fig. 1b. Due to the boundary layer, the fluid particles flowing close to the tube wall have a lower velocity with respect to the fluid flowing in the core of the tube thus they are subject to a lower centrifugal force [23,24]. As a consequence, fluid from the core region is pushed outwards forming a pair of recirculating counter-rotating vortices as presented in Fig. 1c.

In the Reynolds number range of $50 < \mathrm{Re}_{sh} < 10000$ the Nusselt number at shell side can be expressed as [25]

$$\mathrm{Nu}_{sh} = 0.6\mathrm{Re}_{sh}{}^{0.5}\mathrm{Pr}^{0.31} , \tag{1}$$

where Pr is the Prandl number, and for $\mathrm{Re}_{sh} > 10000$

$$\mathrm{Nu}_{sh} = 0.36\,\mathrm{Re}_{sh}^{0.55}\,\mathrm{Pr}^{0.333}\left(\frac{\mu}{\mu_p}\right)^{0.14} , \tag{2}$$

where μ and μ_p are the dynamic viscosity of the wall and fluid, respectively. In shell side flow, Reynolds number is calculated as the mass flow rate, G_{sh}, through equivalent diameter, D_e,

$$\mathrm{Re}_{sh} = \frac{G_{sh}D_e}{\mu_l} . \tag{3}$$

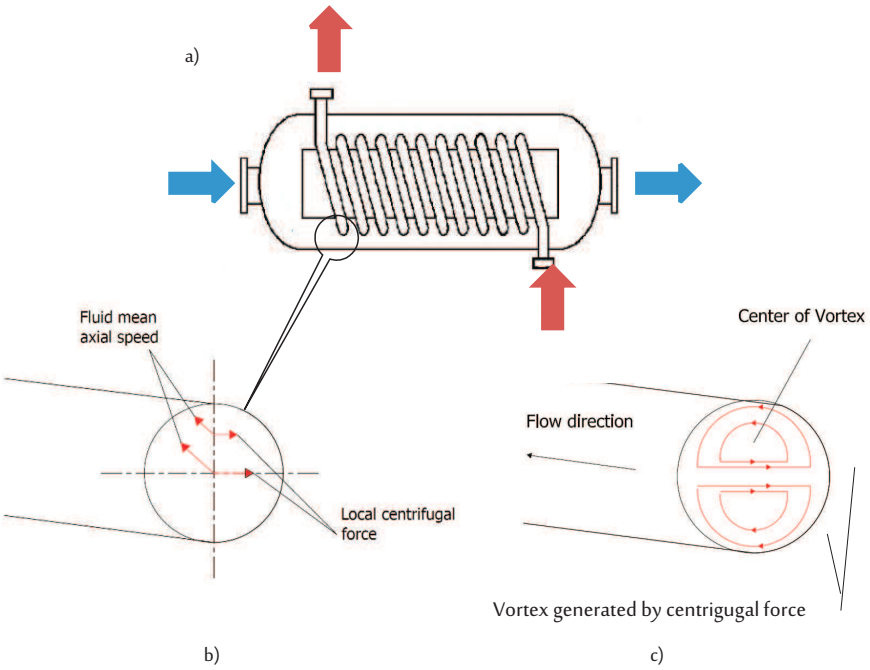

Figure 1: Shell coil heat exchanger view (a), centrifugal force acting on the flowing fluid and axial speed (b), resulting secondary flows (c).

Equivalent diameter depends on the volume of the annulus divided by heat exchanger length and the circumference

$$D_e = \frac{4V_{sh}}{\pi D_0 H} \,. \tag{4}$$

The volume available for the flow of fluid in the annulus, V_{sh}, can be calculated knowing geometrical dimensions of the heat exchanger (Fig. 2 and Tab. 1)

$$V_{sh} = \frac{\pi}{4} C^2 p N - \frac{\pi}{4} {D_0}^2 L \,. \tag{5}$$

Inside the coil, authors decided to use the Dittus-Boelter correlation for dimensionless heat transfer coefficient [26]

$$\mathrm{Nu}_{DB} = 0.023 \mathrm{Re}^{0.8} \mathrm{Pr}^{0.4} \,. \tag{6}$$

Corrected for the coiled tube it becomes

$$\alpha_{io} = \alpha_{DB} \left\{ \left[1 + 3.6 \left(1 - \frac{\delta}{0.5 d_0} \right) \right] \left(\frac{\delta}{0.5 d_0} \right)^{0.8} \right\} \,, \tag{7}$$

where δ is the wall thickness, and α_{DB} means the heat transfer coefficient calculated by Eq. (6), Re is based on inner pipe diameter, d_0, and fluid velocity inside the coil, w_{c-s}

$$\mathrm{Re} = \frac{w_{c-s} d_0}{\nu} \,, \tag{8}$$

where ν is the kinematic viscosity of fluid.

Overall heat transfer coefficient can be calculated as

$$\frac{1}{U} = \frac{1}{\alpha_{sh}} + \frac{1}{\alpha_{i0}} + \frac{\ln\left(\frac{D_0}{d_0}\right)}{2\pi\lambda_{cu} L} + R_t + R_{sh} \,. \tag{9}$$

In present study required heat load was set as $\dot{Q} = 1200$ W. Thus the contact area, A, can be calculated from

$$A = \frac{\dot{Q}}{U\,\mathrm{LMTD}} \,. \tag{10}$$

The logarithmic mean temperature difference LMTD can be used as an average acting temperature gradient between two fluids. It can be written as

$$\mathrm{LMTD} = \frac{(T'_h - T'_c) - (T''_h - T''_c)}{\ln\left(\frac{T'_h - T'_c}{T''_h - T''_c}\right)} \,, \tag{11}$$

where subscripts h and c indicate hot and cold fluids, and superscripts 'prim' and 'double prim' denote temperature at inlet and outlet, respectively.

LMTD is corrected with the fluid correction factor, F

$$\mathrm{LMTD}_{cor} = F\,\mathrm{LMTD} \,. \tag{12}$$

The account for perpendicular flow, the correction factor of 0.99 [7].

The coil heat exchanger has been developed by using values of water properties for average temperature, T_{av}, of cold and hot media. The pressure drop of the heat exchanger for shell and coil side accordingly yields:

$$\Delta P_{sh} = C_D \frac{H}{D_e} \frac{\overline{w}_{s-a}{}^2 \rho}{2} + \sum \zeta \frac{\overline{w}_{s-a}{}^2 \rho}{2} \,, \tag{13}$$

$$\Delta P_{c-s} = f \frac{L}{d_0} \frac{\overline{w}_{a-c}{}^2 \rho}{2} + \sum \zeta \frac{\overline{w}_{a-c}{}^2 \rho}{2} \,, \tag{14}$$

Table 1: Physical assumptions.

Symbol	Unit	Value
r	m	0.02
C	m	0.06
D_0	m	0.006
d_0	m	0.004
d	mm	1
λ_{CU}	W/mK	389

Table 2: Thermal assumptions.

Symbol	Unit	Cold fluid	Hot fluid
m	kg/s	0.01	0.01
T'	°C	15	80
T''	°C	50	60
T_{av}	K	305.65	343.15
C_p	J/kgK	4.18	4.19
Pr	–	5.1	2.55
λ	W/mK	0.619	0.66
μ	Pas	0.000757	0.000404
ρ	kg/m^3	994.87	977.76

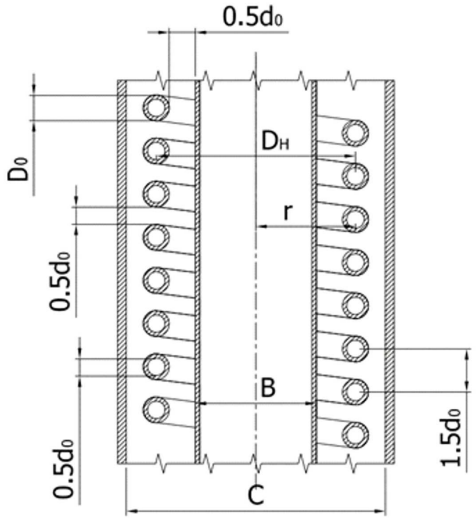

Figure 2: Geometrical assumptions for designed helical heat exchanger.

where ρ is the fluid density and overbar denotes the average velocity.
The friction factor for flow inside the coil can be calculated from relation [22]

$$f = \left[\frac{0.3164}{\mathrm{Re}^{0.25}} + 0.03\left(\frac{d_0}{E}\right)^{1/2}\right]\left(\frac{\mu_w}{\mu}\right)^{0.27}, \tag{15}$$

where μ_w is the dynamic viscosity calculated for wall temperature, factor E dependent on heat exchanger geometrical dimensions, is calculated as

$$E = D_H\left[1 + \left(\frac{p}{\pi D_H}\right)^2\right], \tag{16}$$

where D_H is the average diameter of helix.

Drag coefficient on coil surface was calculated from the Brauer correlation [22]

$$C_D = \frac{0.3164}{\mathrm{Re}^{0.25}} \left[1 + 0.095 \left(\frac{D_0}{D_H} \right)^{1/2} \mathrm{Re}_{sh}{}^{0.25} \right] . \tag{17}$$

Local drag coefficients for Eqs. (13) and (14) were taken from Bell [23] and Achenbach [24].

3 Experimental setup

The main aim of surface modification was to increase turbulization at the outer surface of the coil. As well-known from literature, the heat transfer coefficient at shell side in case of typical helical heat exchangers is smaller than the one at coil side [13].

Figure 3: Obtained construction of helical coils: at the left side – coil made from smooth copper pipe, in the middle – coil with modified surface, at the right side – photo of modified surface.

Both coils have been made by using a small, smooth copper minichannel (see Fig. 3). The average length of channels is 1400 mm and average fin height was equal to 0.5 mm. Each one of built heat exchangers has the same shell construction.

The rig consists of two closed loops of test fluid. The facility was intended to work with any non-chemically aggressive working fluids. In both loops, circulation is forced by electrically powered pumps with a magnetic coupling, capable of providing the mass flow rate from 0.001 to 0.005 g/s and the overpressure up to 0.8 MPa. This type of pumps has been chosen

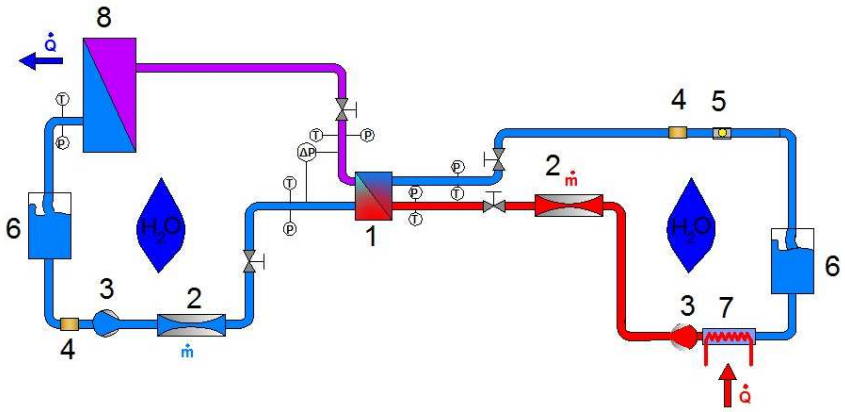

Figure 4: Schematic diagram of experimental rig: 1 – helical coil heat exchanger, 2 – Coriolis mass flow meter, 3 – nonpulsation gear pump, 4 – filter, 5 – inspection glass, 6 – fluid tank , 7 – heater, 8 – chiller.

to provide the circulation of fluid in the test sections and to avoid flow pulsations. Adjustment of the mass flow rate is realized by two independent inverters. Figure 4 presents a schematic diagram of the test facility.

The heat exchanger consists of a copper coiled tube and an insulated shell. The dimensions of the heat exchangers are depicted in Tab. 1. The hot fluid circuit is heated using a thermostatic bath. A pump circulates the hot water in the loop with a preset temperature. A set of valves is used to control the flow rate of cold and hot water, respectively. To measure the flow rates of the cold and hot fluids a Coriolis-type mass flow meters are installed upstream of the heat exchanger. The inlet and outlet temperatures of hot and cold water were recorded using four T-type thermocouples inserted at the inlet and outlet collectors. Also, all the pipes and connections between the temperature measuring stations and heat exchanger were duly insulated. In order to exclude heat capacity of heat exchanger casing from calculations, data points were gathered for steady state conditions. After obtaining constant parameters, temperatures were measured three times with an accuracy of 0.5 °C in the time steps of 20 min, and the average values were used for further analysis. Appropriate arrangements were provided to measure the pressure loss of both tube and shell side. All the tube- and shell-side fluid properties were assessed at the mean temperature of the fluid (average of inlet and outlet temperatures). The measured uncertainty parameters are shown in Tab. 3.

Table 3: Uncertainty of operating parameters.

Parameter	Operating range	Uncertainty
d_0, mm	4	±0.003
D_0, mm	6	±0.003
m, kg/s	0.01–0.03	±0.3%
T, °C	19–92	±0.5
Δp, kPa	0.2–2	±0.075%

4 Data reduction

The hot and cold heat flux are calculated as a product of water mass flux, water specific heat capacity and the inlet-outlet water temperature difference:

$$\dot{Q}_c = c_p m_c (T_{c,out} - T_{c,in}) \,, \tag{18}$$

$$\dot{Q}_h = c_p m_h (T_{h,in} - T_{h,out}) \,. \tag{19}$$

The measured pressure drop is the sum of friction pressure drop, and expansion and contraction losses due to the headers at both ends of the test section

$$\Delta P_{measured} = \Delta P_{frict} + \Delta P_{\text{exp}} + \Delta P_{con} \,. \tag{20}$$

The pressure drop due to contraction was estimated using a flow model recommended by Hewitt *et al.* [26] for single phase flow.

$$\Delta P_{con} = \frac{G^2}{2\rho} \left[\left(\frac{1}{C_{con}} - 1 \right) + 1 - \gamma^2 \right] \,, \tag{21}$$

where γ is the area ratio ($A_{test-section}/A_{header}$) and C_{con} is the coefficient of contraction, which is, in turn, a function of this area ratio,

$$C_{con} = \frac{1}{0.639(1-\gamma)^{0.5} + 1} \,. \tag{22}$$

For the expansion into the header from the test section, the following flow model recommended by Hewitt *et al.* [27] was also used:

$$\Delta P_{\text{exp}} = \frac{G^2 \gamma (1-\gamma) \psi_s}{\rho} \,, \tag{23}$$

where ψ is the separated flow multiplier, while is also a function of the phase densities and the quality. In single flow case, those multiplier and quality are equal to unity.

The number of transfer units, NTU, is calculated as

$$\text{NTU} = \frac{UA}{W_{min}} \tag{24}$$

where U is the overall heat transfer coefficient and A is the heat transfer surface area of the heat exchanger,

$$W_{min} = min\ (W_c, W_h)\ , \tag{25}$$

where W_c and W_h are the heat capacity rates of the cold and hot fluids, respectively. In heat exchanger analysis, it is also convenient to define another dimensionless quantity called the capacity ratio as

$$W = \frac{W_{min}}{W_{max}}\ , \tag{26}$$

where W_{max} is the higher of the two considered capacities.

The heat transfer effectiveness is defined as actual heat transfer rate to maximum possible heat transfer:

$$\varepsilon = \frac{\dot{Q}}{\dot{Q}_{max}}\ . \tag{27}$$

The actual heat transfer rate in a heat exchanger can be determined from an energy balance on the hot or cold fluids and can be expressed as

$$\dot{Q} = W_c(T_{c,out} - T_{c,in}) = W_h(T_{h,in} - T_{h,out})\ . \tag{28}$$

To determine the maximum possible heat transfer rate in a heat exchanger, we first recognize that the maximum temperature difference in a heat exchanger is the difference between the inlet temperatures of the hot and cold fluids

$$\Delta T_{max} = T_{h,in} - T_{c,in}\ . \tag{29}$$

Therefore, the maximum possible heat transfer rate in a heat exchanger is

$$\dot{Q}_{max} = W_{min}(T_{h,in} - T_{c,in})\ , \tag{30}$$

where W_{min} is the lower heat capacity of cold and hot fluid.

Experimental values of Nusselt number, Nu, at shell side and coil side were calculated as

$$\mathrm{Nu}_{\mathrm{exp}\_sh} = \frac{\alpha_{\mathrm{exp}\_sh} D_e}{\lambda} , \tag{31}$$

$$\mathrm{Nu}_{\mathrm{exp}\_c-s} = \frac{\alpha_{\mathrm{exp}\_c-s} d_0}{\lambda} . \tag{32}$$

The Dean number, D, is a dimensionless group in fluid mechanics, which occurs in the study of flow in curved pipes and channels (Fig. 2):

$$\mathrm{D} = \frac{\rho w d_0}{\mu} \left(\frac{d_0}{2r} \right)^{\frac{1}{2}} , \tag{33}$$

$$U = \frac{1}{\dfrac{1}{\alpha_{\mathrm{exp}\alpha\_sh}} + \dfrac{1}{\alpha_{\mathrm{exp}\alpha\_i0}} + \dfrac{\ln\left(\frac{D_0}{d_0}\right)}{2\pi\lambda_{CU} L}} . \tag{34}$$

5 Experimental results

In order to estimate the influence of surface modifications on flow through the heat exchanger, as the first step of experimental validation hydraulic performance of heat exchanger was examined. Because only coil external surface was modified only shell side flow was investigated in detail for both reference and modified geometry.

As can be seen in Fig 5. there is no significant difference between the hydraulic characteristic of plain and modified helical coil heat exchanger. It should be noted also that the predicted value of pressure drop with Eq. (13) has good agreement with experimental results, but it tends to over predict ΔP values for higher flow rates. As well as pressure drop in shell side the experimental data for pressure drop at coil side was compared with the prediction given by Eq. (14). Figure 6 clearly presents acceptable agreement between predictions and experimentally obtained results.

Figure 7 presents' linear regression values for experimental series grouped in constant shell side fluid velocities (cold). The resulting heat transfer coefficient of cold fluid from experimental data was calculated based on Wilsons plot method [3]. The heat transfer coefficient was calculated for the tube thickness of 1 mm. The tube material (copper) has the thermal conductivity, λ, equal to 389 W/mK. It has to be noted that overall heat transfer coefficient generally is larger for the modified construction of heat

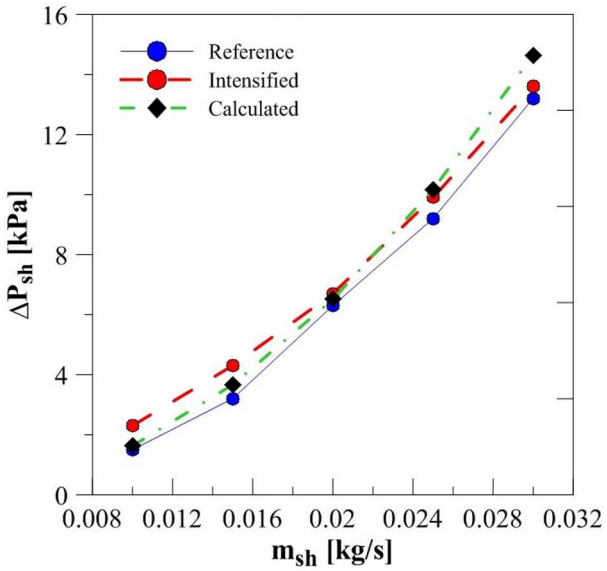

Figure 5: Pressure drops in shell side as a function of mass flow rate.

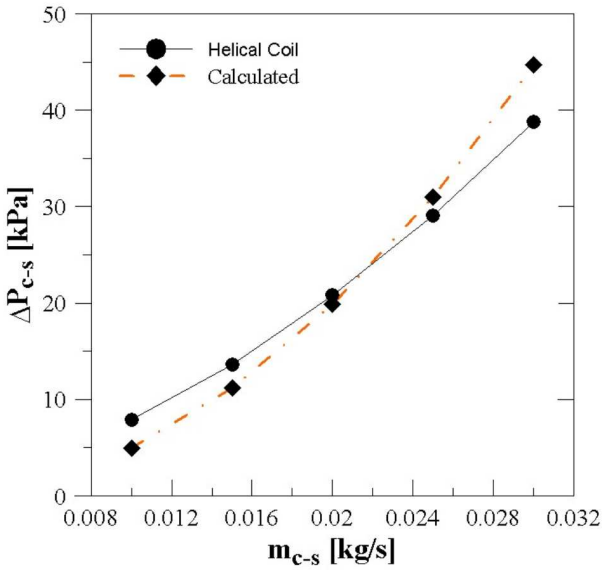

Figure 6: Pressure drops in coil side as a function of mass flow rate.

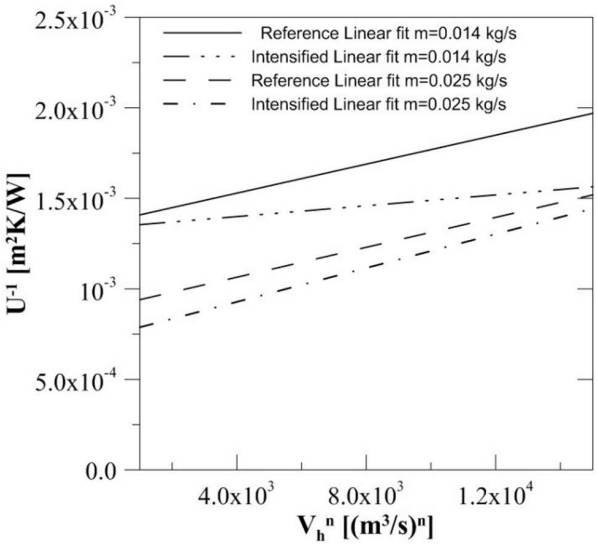

Figure 7: Linear regression of experimental data for calculating heat transfer coefficient by Wilsons plot method, for varying hot and constant cold fluid mass flow rate in case of countercurrent flow.

exchanger. But the difference is quite small. The low values for the small flow velocities could also be due to the nature of the Wilson plots. It was noted that small changes in the coefficients used in the Wilson plots had a small effect on the inner Nusselt numbers, but much larger effects on the annulus Nusselt numbers. So the Wilson plots may be part of the reason for the divergence between the experimental and predicted values.

Based on a comparison of theoretical values of Nusselt numbers and experimental results a good agreement of used correlations can be stated. The differences at shell side and coil side are not larger than 30%. Results were shown in Figs. 8 and 9. As was expected based on analytical modeling of coil heat exchanger the Nusselt number for coil side are clearly larger than the shell side. Considering pressure drop at shell side are also significantly smaller than at the coil side.

Figure 10 represents the variations of Nusselt number versus Dean number for three different water inlet temperatures at shell side and at coil side for reference heat exchanger construction. It is important to notice that increment of water temperature reduces obtained Nusselt numbers at shell side, especially in the low Dean number region. Unfortunately for coil side the difference is so small than even after zoom experimental points, it is

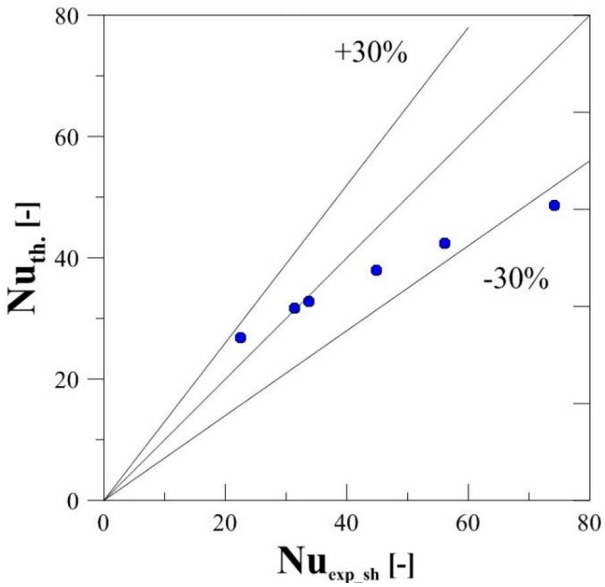

Figure 8: Comparison of experimental and theoretical Nusselt number for shell side in case of the unmodified surface.

negligible. It is also seen that at higher temperatures, the range of Dean number is greater as a result of lower water viscosity.

One of the most common methods to compare the various types of heat exchangers is to use ε-NTU methodology [28–30]. Collected experimental data for co- and countercurrent flow configuration in each of presented heat exchangers allow verifying the influence of temperature field on heat transfer coefficient. Figures 11 and 12 show the effectiveness of coil heat exchangers calculated using Eq. (27) as a function of a number of transfer units. In both cases, countercurrent flow configuration with hot water inside the coil is the most effective.

The heat exchanger with surface modification on average has the largest effectiveness from all of the considered operational conditions. Instead of that fact it should be noticed that generally the difference between the effectiveness of both heat exchangers wasn't significant.

Figure 13 indicates that the effectiveness of the heat exchanger decreases with the increase in Dean number inside tube in case of reference and intensified heat exchangers. From the plot, it is also evident that for higher water flow rates inside the tube, effectiveness is almost constant in all cases. The analysis also indicates that the effectiveness of the helical

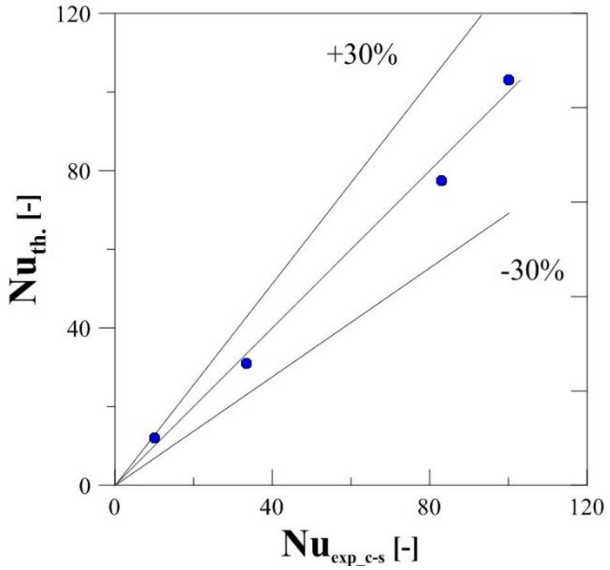

Figure 9: Comparison of experimental and theoretical Nusselt number for coil side in case of the unmodified surface.

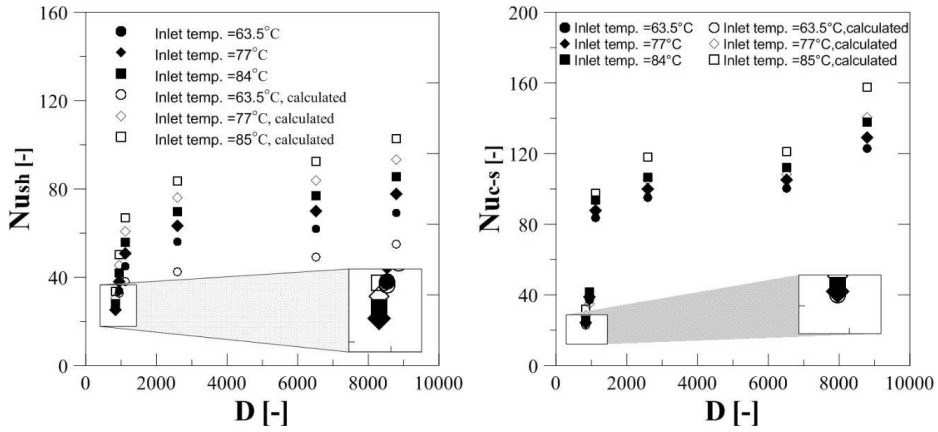

Figure 10: Variation of Nusselt number with Dean number for different fluid inlet temperature in case of unmodified surface: a) for shell side, b) for coil side.

coiled configuration is highest in case 'b)', for spiral coiled with external surface modification. Parallel flow configuration results with the effective-

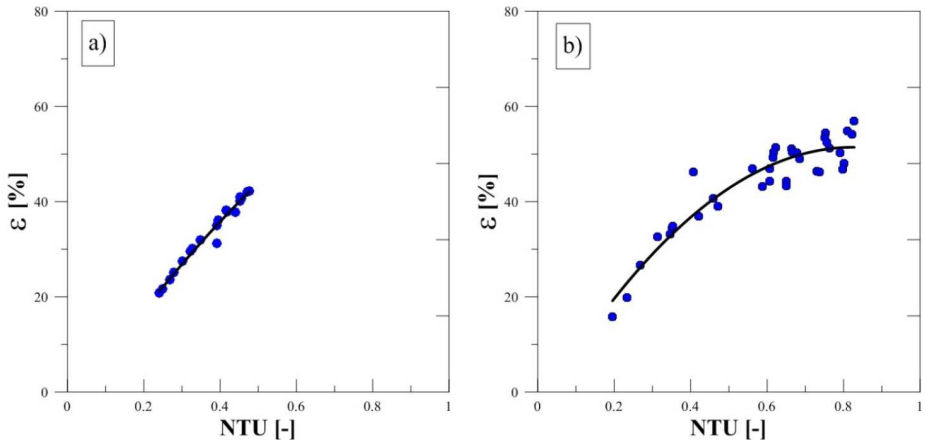

Figure 11: Experimentally obtained reference heat exchanger effectiveness in function of NTU for: a) parallel flow configuration, b) counter-flow configuration.

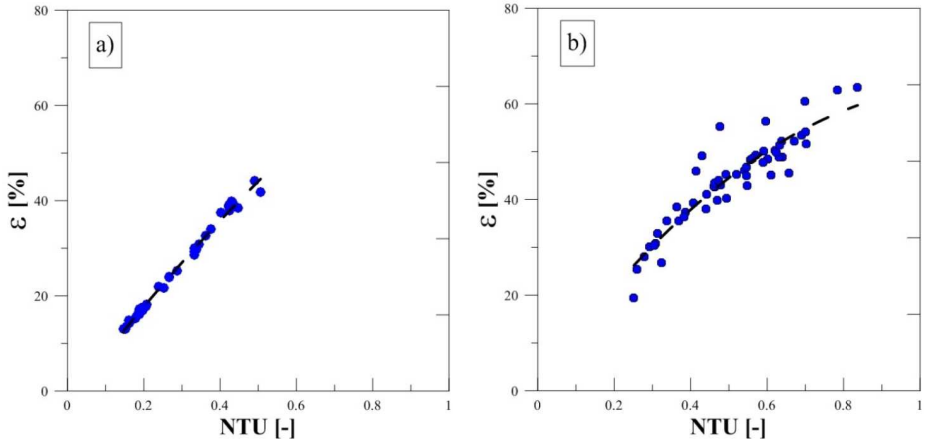

Figure 12: Experimentally obtained modified heat exchanger effectiveness in function of NTU for: a) parallel flow configuration, b) counter-flow configuration.

ness of intensified heat exchanger lower about 5% than reference type, but for lower mass flow rates. This can be explained by measurement error which is higher for lower flow rates.

Counterflow configuration also depicts similar effectiveness for low flow rates, but significantly larger for Dean numbers above 3000. In authors, opinion difference in results may be explained by entrance effects in both heat exchangers. For parallel flow at the inlet of heat exchanger heat is

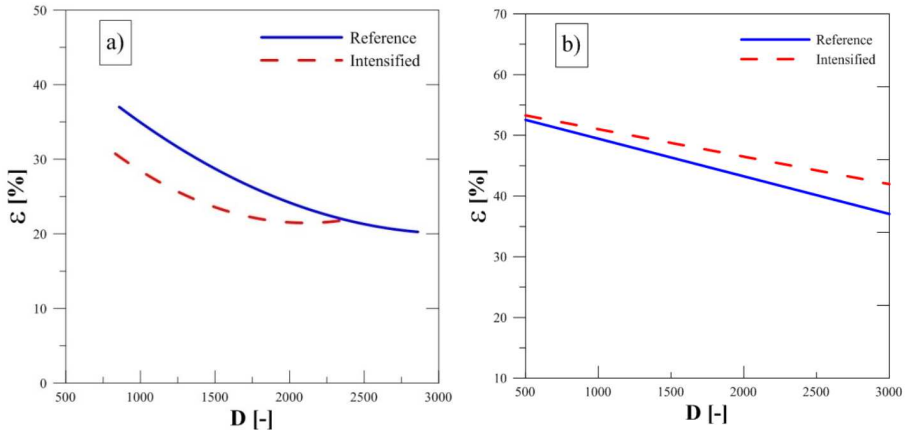

Figure 13: Effectiveness of helical coils heat exchanger, as a function of the Dean number (D): a) parallel flow configuration, b) counter-flow configuration.

transferred due to the large temperature difference, also heat transfer coefficient is enhanced due to inlet effects, therefore surface enhancement does not play a significant role in it. Afterward with lower temperature difference in heat exchanger, enhancement of heat transfer coefficient falls within the measurement error. On another hand for counter flow configuration, working fluids have similar temperature gradient along the flow path, therefore after inlet effects are suppressed, modified surface offers heat transfer enhancement that is measurable due to the higher temperature difference.

6 Conclusions

Authors presented and successfully implemented, a simple mathematical methodology to model the shell and coil heat exchanger. In this paper, results show a comparison between helically coiled heat exchanger with surface modification by means of micro fins. During the experiments the mass flow rate in the inner tube and the annulus were both varied, both the counter and parallel flow configuration was tested. The experimental values of heat transfer coefficient have been obtained by the Wilson plot method.

It was observed that the overall heat transfer coefficient increases with increase in the inner coiled tube Dean number for a constant flow rate in the annulus region. Similar trends in the variation of overall heat transfer

coefficient were observed for different flow rates in the annulus region for a constant flow rate in the inner coiled tube. It was shown that obtained average Nusselt numbers for the shell side have increased with surface modifications.

The literature predictions for hydrodynamics and fully developed heat transfer were in good agreement with experimental results. The agreement with the numerical and experimental predictions of Nusselt number values was well within 30%.

As was expected based on presented above facts the heat exchanger with surface modification on average has larger effectiveness than reference construction.

Received 20 June 2016

References

[1] Muszynski T. Kozieł S.M.: *Parametric study of fluid flow and heat transfer over louvered fins of air heat pump evaporator*. Arch. Thermodyn. **37**(2016), 3, 41–58, DOI:10.1515/aoter-2016-0019.

[2] Muszynski T., Andrzejczyk R.: *Heat transfer characteristics of hybrid microjet – Microchannel cooling module*. Appl. Therm. Eng. **93**(2016), 1360–1366, DOI:10.1016/j.applthermaleng.2015.08.085.

[3] Muszynski T., Andrzejczyk R.: *Applicability of arrays of microjet heat transfer correlations to design compact heat exchangers*. Appl. Therm. Eng. **100**(2016), 105–113, DOI:10.1016/j.applthermaleng.2016.01.120.

[4] Rozzi S., Massini R., Paciello G., Pagliarini G., Rainieri S., Trifiro A.: *Heat treatment of fluid foods in a shell and tube heat exchanger: Comparison between smooth and helically corrugated wall tubes*. J. Food Eng. **79**(2007) 249–254, DOI:10.1016/j.jfoodeng.2006.01.050.

[5] Jayakumar J.S., Mahajani S.M., Mandal J.C., Vijayan P.K., Bhoi R.: *Experimental and CFD estimation of heat transfer in helically coiled heat exchangers*. Chem. Eng. Res. Des. **86**(2008), 221–232, DOI:10.1016/j.cherd.2007.10.021.

[6] Berger S.A., Talbot L., Yao L.S.: *Flow in curved pipes*. Annu. Rev. Fluid Mech. **15**(1983), 461–512.

[7] Kakaç S., Shah R.K., Aung W.: *Handbook of single-phase convective heat transfer*. Wiley New York *et al.*, 1987.

[8] Naphon P., Wongwises S.: *A review of flow and heat transfer characteristics in curved tubes*. Renew. Sustain. Energy Rev. **10** (2006), 463–490, DOI:10.1016/j.rser.2004.09.014.

[9] Lin C.X., Zhang P., Ebadian M.A.: *Laminar forced convection in the entrance region of helical pipes*. Int. J. Heat Mass Transf. **40**(1997), 3293–3304.

[10] Kumar V., Faizee B., Mridha M., Nigam K.D.P.: *Numerical studies of a tube-in- tube helically coiled heat exchanger*. Chem. Eng. Process. Process Intensif. **47**(2008), 2287–2295.

[11] Conte I., Peng X.F.: *Numerical investigations of laminar flow in coiled pipes*. Appl. Therm. Eng. **28**(2008), 423–432.

[12] Patankar S.V., Pratap V.S., Spalding D.B.: *Prediction of laminar flow and heat transfer in helically coiled pipes*. J. Fluid Mech. **62**(1974), 539–551.

[13] Jamshidi N., Farhadi M., Ganji D.D., Sedighi K.: *Experimental analysis of heat transfer enhancement in shell and helical tube heat exchangers*. Appl. Therm. Eng. **51**(2013), 644–652, DOI:10.1016/j.applthermaleng.2012.10.008.

[14] Xin R.C., Awwad A., Dong Z.F., Ebadian M.A.: *An experimental study of single-phase and two-phase flow pressure drop in annular helicoidal pipes*. Int. J. Heat Fluid Flow. **18**(1997), 482–488.

[15] Petrakis M.A., Karahalios G.T.: *Exponentially decaying flow in a gently curved annular pipe*. Int. J. Non. Linear. Mech. **32**(1997), 823–835.

[16] Petrakis M.A., Karahalios G.T.: *Fluid flow behaviour in a curved annular conduit*. Int. J. Non. Linear. Mech. **34**(1999), 13–25.

[17] Di Liberto M., Ciofalo M.: *A study of turbulent heat transfer in curved pipes by numerical simulation*. Int. J. Heat Mass Transf. **59**(2013), 112–125.

[18] Moawed M.: *Experimental study of forced convection from helical coiled tubes with different parameters*. Energy Convers. Manag. **52**(2011), 1150–1156.

[19] Designing_Helical_Coil_Heat Exgr_1982.pdf.

[20] Ankanna B.C., Reddy B.S.: *Performance analysis of fabricated helical coil heat exchanger*. Int. J. Eng. Res. **3**(2014), Iss. 1, 33–39.

[21] Kast W., Gaddis E.S., Wirth K.-E., Stichlmair J.: *L1 Pressure Drop in Single Phase Flow*. In: VDI Heat Atlas, Springer, 2010, 1053–1116.

[22] Brauer H.: *Strömungswiderstand und Wärmeübergang bei quer angeströmten Wärmeaustauschern mit kreuzgitterförmig angeordneten glatten und berippten Rohren*. Chemie Ing. Tech. **36** (1964) 247–260, DOI:10.1002/cite.330360314 (in German).

[23] Bell K.J.: *Delaware Method for Shell-side Design*. Taylor & Francis, New York 1988.

[24] Achenbach E.: *Investigations on the flow through a staggered tube bundle at Reynolds numbers up to Re = 107*. Wärme-Und Stoffübertragung. **2**(1969), 47–52.

[25] Lazova M., Huisseune H., Kaya A., Lecompte S., Kosmadakis G., De Paepe M.: *Performance evaluation of a helical coil heat exchanger working under supercritical conditions in a solar organic Rankine cycle installation*. Energies. **9**(2016), 432, DOI:10.3390/en9060432.

[26] Jo D., Al-Yahia O.S., Altamimi R.M., Park J., Chae H.: *Experimental investigation of convective heat transfer in a narrow rectangular channel for upward and downward flows*. Nucl. Eng. Technol. **46**(2014), 2, 195–206, DOI:10.5516/NET.02.2013.057.

[27] Hewitt G.F., Shires G.L., Bott T.R.: *Process Heat Transfer*. CRC press Boca Raton, FL, 1994.

[28] Muszynski T.: *Design and experimental investigations of a cylindrical micro-jet heat exchanger for waste heat recovery systems*. Appl. Therm. Eng. (2017), DOI:10.1016/j.applthermaleng.2017.01.021.

[29] Laskowski R.: *The concept of a new approximate relation for exchanger heat transfer effectiveness for a cross-flow heat exchanger with unmixed fluids*. J. Power Technol. **91**(2011), 93–101.

[30] Cieśliński J.T., Fiuk A., Typiński K., Siemieńczuk B.: *Heat transfer in plate heat exchanger channels: Experimental validation of selected correlation equations*. Arch. Thermodyn. **37**(2016), 3, 19-29, DOI:10.1515/aoter-2016-0017.